Dynamics of the Disks of Nearby Galaxies

B. Fuchs

Astronomisches Rechen-Institut am Zentrum für Astronomie der Universität Heidelberg,
Mönchhofstr. 12-14, 69120 Heidelberg, Germany

Received 2008, accepted 2008
Published online later

Key words Galaxies: kinematics and dynamics

I describe how the dynamics of galactic disks can be inferred by imaging and spectroscopy. Next I demonstrate that the decomposition of the rotation curves of spiral galaxies into the contributions by the various components of the galaxies is highly degenerate. Constraints on the decomposition can be found by considering implications for the dynamics of the galactic disks. An important diagnostic is the Toomre Q stability parameter which controls the stability of a galactic disk against local Jeans collapse. I also show how the density wave theory of galactic spiral arms can be employed to constrain the mass of a galactic disk. Applying both diagnostics to the example of NGC 2985 and discussing also the implied mass-to-light ratio I demonstrate that the inner parts of the galaxy, where the optical disk resides, are dominated by baryons. When I apply this method to the disks of low surface brightness galaxies, I find unexpectedly high mass-to light ratios. These could be explained by population synthesis models which assume a bottom heavy initial mass function similar to the recently proposed 'integrated galactic initial mass function'.

© 2006 WILEY-VCH Verlag GmbH & Co. KGaA, Weinheim

arXiv:0810.3503v1 [astro-ph] 20 Oct 2008

1 Introduction

The dynamics of the disks of spiral galaxies is inferred from observations of the kinematics of the stars and the interstellar gas in the galactic disks. The most immediate way is to measure the mean rotation of the stars and the gas around the galactic center. Since the pioneering work of Rubin et al. (1978) rotation curves of galaxies have been observed by long slit spectroscopy in optical filter bands in great numbers. The rotation curves are usually derived using emission lines which are emitted by HII regions in the spiral arms of the galaxies. In Fig. 1 I reproduce a part of a long slit spectrum of NGC 6070 close to the H_β line (Fried & Fuchs, unpublished). The rotation curve – not yet corrected for inclination – is clearly visible to the naked eye. Optical rotation curves reach radially outwards typically to three radial exponential scale lengths of the disks.

Rotation curves observed by 21 cm emission from the interstellar HI, on the other hand, can usually be traced radially much further outwards. In their pioneering work on NGC 3198 van Albada et al. (1985) could observe the HI rotation curve out to nearly 12 optical radial scale lengths and confirmed the existence of dark matter halos around spiral galaxies beyond any reasonable doubts. Rotation curves of both kinds are now available in large numbers and are compiled in catalogues like that of Prugniel et al. (1998).

In contrast to the mean velocities velocity dispersions are technically much more difficult to measure. The observed stellar absorption lines have to be deconvolved with the corresponding lines of template stars to measure line broadenings due to velocity dispersions of a few tens of km/s. Moreover spectra at at least two slit positions along the major and minor axes are required to disentangle the three components of the velocity dispersions in the radial, tangential and vertical directions, respectively. This disentanglement is greatly facilitated by the fact that the ratio of radial to tangential velocity dispersion can be related by epicyclic orbit theory (Lindblad 1959) to the shape of the rotation curves and need not to be measured directly[1]. Early results were presented in the work of Bottema (1993). However, given the technical possibilities of that time his results have too large errors to be used for the purposes described below. More reliable data have been obtained by Gerssen et al. (1997, 2000) for the two galaxies NGC 488 and NGC 2985. Recently the disk mass project (Verheijen et al. 2004) has begun to measure the velocity dispersions of face-on galaxies with the accurate Pmass instrument.

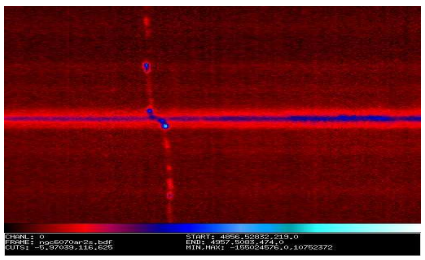

Fig. 1 Long slit spectrum of NGC 6070 near the H_β emission line. The dispersion of the spectrograph is oriented horizontally, while the slit direction points vertically.

[1] $\sigma_U/\sigma_V = 2\Omega/\kappa$ to be precise.

WILEY InterScience® DISCOVER SOMETHING GREAT

© 2006 WILEY-VCH Verlag GmbH & Co. KGaA, Weinheim

2 Modelling rotation curves

Rotation curves are modelled by constructing mass models of the observed galaxies. These include usually a disk with an exponential density profile characterized by the central surface density and a radial scale length, a bulge model of the de Vaucouleurs or Sérsic type characterized by the central density and the half-light-radius, and a model for the dark halo either with a NFW density distribution profile (Navarro et al. 1997),

$$\rho(r) = \frac{\rho_0}{r(r_\mathrm{c}+r)^2}, \tag{1}$$

or a quasi-isothermal sphere

$$\rho(r) = \frac{\rho_0}{r_\mathrm{c}^2+r^2}. \tag{2}$$

As can be seen form eqns. 1 and 2 the NFW law has a central density cusp, whereas the quasi-isothermal sphere has a central homogeneous core. Assuming essentially circular orbits of the stars and the interstellar gas around the galactic center - which is actually inadequate close to the center - the centripetal acceleration due to gravity is balanced by the centrifugal acceleration. For spherical systems like the bulge or the dark halo this simply means

$$\frac{\upsilon_\mathrm{c}^2}{r} = \frac{GM(<r)}{r^2}, \tag{3}$$

with G denoting the constant of gravitation, whereas for a flat exponential disk the circular velocity is given by Freeman's (1970) formula. The actual rotation curve of the galaxy is then given by the sum of three terms

$$\upsilon_\mathrm{c}(r) = \sqrt{\upsilon_\mathrm{b}^2(r)+\upsilon_\mathrm{d}^2(r)+\upsilon_\mathrm{h}^2(r)}, \tag{4}$$

However, the decomposition of a rotation curve into its three components is notoriously degenerate. I demonstrate this again with the famous example of NGC 3198 which has a radial exponential scale length of r_d = 2.6 kpc. In Fig. 2 the rotation curve is fitted by a maximum disk model, i.e. the disk contribution is chosen as high as allowed by the data. Fig. 3 shows a model with a submaximal disk, now of course with different halo parameters. Both fits cannot be distinguished by goodness-of-fit tests from each other, but further constraints on the mass of the disk are needed. I have suggested for some time (Fuchs 1999) that the implied internal dynamical state of the stellar disks according to the galaxy models might provide such constraints.

3 Dynamical stability of galactic disks

In a rotating self gravitating disk of stars there is an interplay of gravity, pressure, and rotation. Patches of the disk become Jeans unstable on scales larger than the Jeans length

$$\lambda \geq \lambda_\mathrm{J} = \frac{\sigma^2}{G\Sigma}, \tag{5}$$

where σ denotes the velocity dispersion of the stars and Σ is the surface density of the disk. Detailed conservation of angular momentum sets, on the other hand, an upper limit on the scales on which density perturbations can grow,

$$\lambda \leq \lambda_\mathrm{c} = \frac{G\Sigma}{\Omega^2}, \tag{6}$$

where Ω denotes the angular frequency of the patch under consideration. If the 'upper' limit is lower than the 'lower' limit, $\lambda_\mathrm{c} < \lambda_\mathrm{J}$, growth of density perturbations is suppressed on all scales. More precisely this means that the Toomre (1964) stability parameter,

$$Q = \frac{\kappa\sigma_\mathrm{U}}{3.36G\Sigma}, \tag{7}$$

must be larger than 1 to ensure that a thin galactic disk is stable against exponentially growing density perturbations. In eq. 7 κ denotes the epicyclic frequency of the stellar orbits,

$$\kappa = \sqrt{2}\,\frac{\upsilon_\mathrm{c}}{r}\sqrt{1+\frac{r}{\upsilon_\mathrm{c}}\frac{\mathrm{d}\upsilon_\mathrm{c}}{\mathrm{d}r}}, \tag{8}$$

and σ_U the radial velocity dispersions of the stars. The coefficient 3.36 applies to a Schwarzschild velocity distribution of the stars; in the case of an isothermal gas it is replaced by π. If $Q < 1$, this represents a serious threat to the fate of a galactic disk. In one of earliest numerical simulations of the evolution of a self-gravitating rotating disk Hockney & Hohl (1969) could already show that a thin $Q < 1$ disk

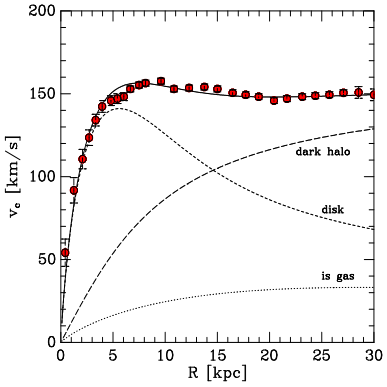

Fig. 2 Maximum disk decomposition of the rotation curve of NGC 3198. The contributions due to the stellar disk, the interstellar gas, and the dark halo are indicated.

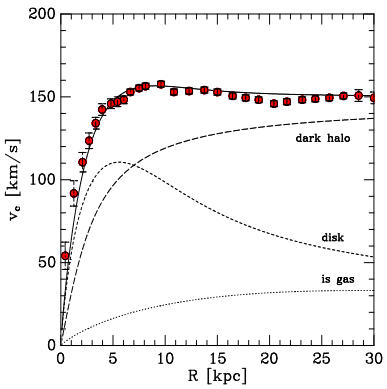

Fig. 3 Submaximal disk decomposition of the rotation curve of NGC 3198.

© 2006 WILEY-VCH Verlag GmbH & Co. KGaA, Weinheim

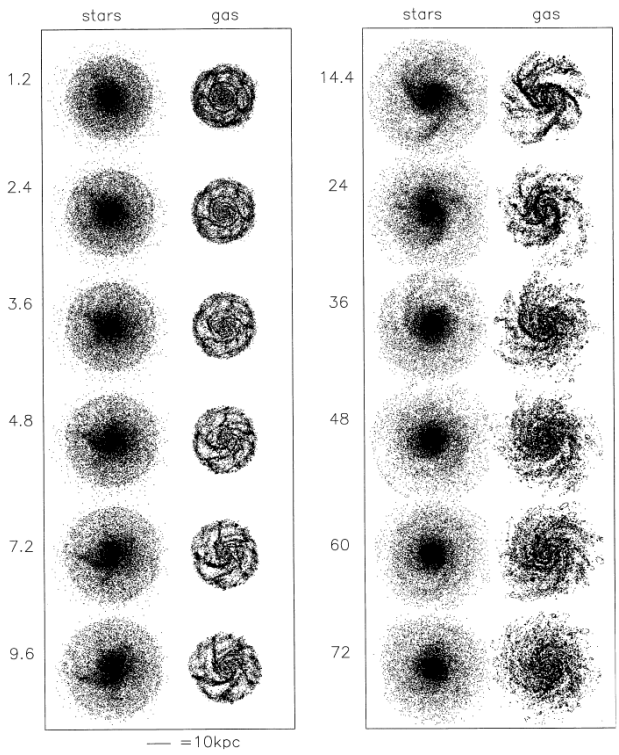

Fig. 4 Snapshots of a numerical simulation of the evolution of a combined disk of stars and gas. The disks are set up initially in radial force equilibrium and with Toomre parameters $Q_* = 1.5$ and $Q_g = 0.5 - 0.7$ respectively. Time is given in units of 10^7 yrs.

undergoes, even if it is rotating fast enough that the gravitational and centrifugal forces are in equilibrium, so violent instabilities that it eventually disintegrates. A $Q = 1$ disk, on the other hand, develops strong non-axisymmetric structures, but stays essentially intact. More recently Fuchs & v. Linden (1998) have run numerical simulations of the evolution of a combined star and gas disk. Snapshots of one of these simulations are shown in Fig. 4. Initially the combined disk was set up in radial force equilibrium and with Toomre parameters Q_* = 1.5 and Q_g = 0.5 - 0.7. Such a disk has an effective Q parameter of slightly less than 1. The disk became immediately unstable as witnessed by the ring like structures especially in the gas disk. The rings fragment into clumps and shear then due to the differential rotation into spiral arms. These grow then rapidly to large amplitudes, both in the stellar and gas disks. The perturbations become so strong that they heat up the stellar disk dynamically so much that all spiral structures are eventually wiped out in it. A disk with $Q < 1$ is not an equilibrium model!

The physical reason that galactic disks are prone to such fierce gravitational instabilities lies in their thin geometry. One can imagine a disk as an assembly of thin rings. The gravitational attraction does not vanish inside the ring like in a spherical shell, but diverges to infinite repulsion at the inner edge. At the outside edge of the ring the gravitational attraction becomes infinite regardless of the actual surface

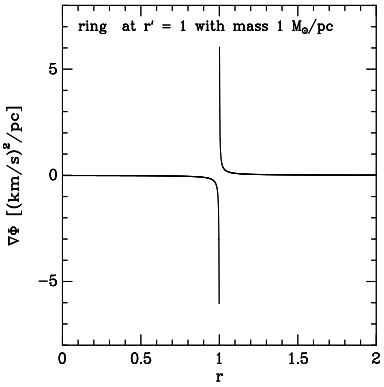

Fig. 5 The radial gravitational force of a mass loaded thin ring calculated in the plane of the ring. The forces diverge at the edges of the ring.

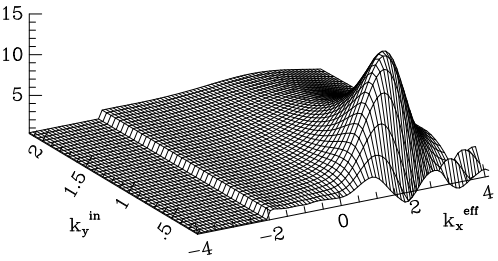

Fig. 6 Amplification factor of the swing-amplification mechanism for spiral density waves. The amplification factor is shown as function of the circumferential wave number k_y and the radial wave number k_x, both measured in units of $k_{\rm crit}$, assuming a flat rotation curve, $A = \Omega/2$. Peak amplification occurs at $k_y = 0.5\,k_{\rm crit}$.

density of the ring. In Fig. 5 I illustrate an example. An assembly of such mass loaded rings must be obviously a highly unstable system.

4 Density wave theory of spiral arms.

The density wave theory predicts the preferential wave length λ of spiral density waves. I adopt here the concept of swing-amplification theory (Toomre 1981) which predicts

$$\lambda = \mathcal{X}(A/\Omega)\,\lambda_{\rm crit} \tag{9}$$

with the natural length unit

$$\lambda_{\rm crit} = \frac{4\,\pi^2 G\,\Sigma}{\kappa^2}. \tag{10}$$

The coefficient $\mathcal{X}$ in eq. 9 depends on the slope of the rotation curve measured by Oort's constant $\frac{A}{\Omega} = -\frac{1}{2}\frac{r}{\Omega}\frac{{\rm d}\Omega}{{\rm d}r}$. In Fig. 6 I reproduce a figure of the operation characteristics of the swing-amplification mechanism taken from Fuchs (2001). The amplification factor is shown as function of the circumferential wave number $k_{\rm y} = 2\,\pi/\lambda$ and the radial wave number $k_{\rm x}$ assuming a flat rotation curve, $A = \Omega/2$. As can be seen amplification becomes maximal at $k_{\rm x}$ around 2 and 3 $k_{\rm crit}$($k_{\rm crit} = 2\,\pi/\lambda_{\rm crit}$). Peak amplification occurs in this example of a flat rotation curve at $k_{\rm y} = 0.5$ or $\lambda = 2\lambda_{\rm crit}$. A

© 2006 WILEY-VCH Verlag GmbH & Co. KGaA, Weinheim

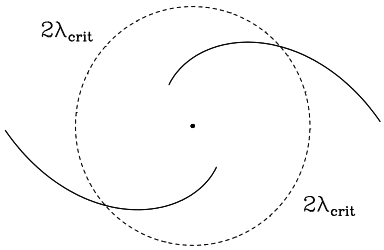

Fig. 7 Sketch of how the preferred wave length – $2\,\lambda_{crit}$ in this example – is related to the number of spiral arms.

relation for the coefficient $\mathcal{X}(A/\Omega)$ for other slopes of the rotation curve is given in Fuchs (2001).

Athanassoula et al. (1987) have pointed out that eq. 9 can be used to constrain the mass of the disk of a spiral galaxy. In Fig. 7 I illustrate with a sketch how the circumferential wave length is related to the number of spiral arms m. Obviously the number of arms is determined by how often the preferred wave length fits onto the annulus,

$$m = \frac{2\,\pi\,r}{\lambda} = \frac{2\,\pi\,r}{\mathcal{X}\lambda_{\rm crit}}. \qquad (11)$$

Thus one can infer from the number of spiral arms m, if the rotation curve is known, the critical wave length $\lambda_{\rm crit}$, and from thence the surface density Σ (cf. eq. 10). This concept has been tested successfully with numerical simulations of the spiral structure of galactic disks. Since the parameters of the disk which have been adopted for the simulation are known, one can read eq. 11 from right to left and compare the predicted and actually found number of spiral arms. For instance, in the simulation by Fuchs & v. Linden (1998) the predicted number of spiral arms is m = 3 which can be clearly confirmed in the snapshot at t = 14.4·10^7 yrs in Fig. 4.

Often it is argued that spiral density waves do not grow spontaneously in the disks of galaxies, but are induced by tidal forces during encounters of two galaxies. Such events do occur, but are not long lived. Zang & Toomre (Toomre 1981) have demonstrated with their work on the Mestel disk that such induced spiral density waves wrap up and die out on the timescale of one galactic revolution. Similarly Dubinski et al. (2008) have shown that in their numerical simulations satellite galaxies orbiting around galaxies induce in the galactic disks of the parent galaxies transient, swing amplified density waves.

5 Example: Diagnostics of NGC 2985

NGC 2985 is a nearby (D = 18 Mpc) bright spiral galaxy. An image taken from DSS, which is reproduced in Fig. 8, shows that it has developed well defined bisymmetric spiral arms. Gerssen et al. (2000) have measured its rotation curve and the velocity dispersions of the stars in two slit positions so that the three dimensional velocity dispersion components are available. Moreover, they have imaged the galaxy and derived its surface density profile which is shown in Fig. 9.

Fig. 8 Image of NGC 2985. (Source: DSS)

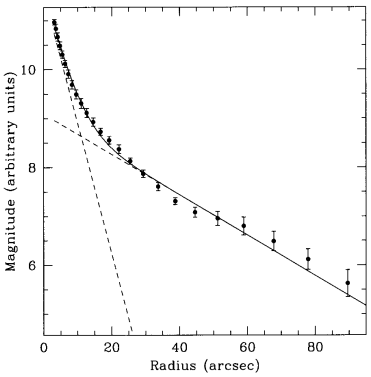

Fig. 9 Surface density profile of NGC 2985. The dashed lines are fits of the bulge and the exponential disk, respectively. The solid line is the superposition of both components.

The authors have also provided a bulge-disk model for the photometry by fitting a bulge with an exponential density profile and an exponential disk with a radial scale length of $r_{\rm d}$ = 2.6 kpc to their data. Arifyanto & Fuchs (2001) have changed this model slightly. They modelled the bulge by a softened power law, $\rho \sim (r_{\rm c}^2 + r^2)^{-1.75}$ with $r_{\rm c}$ = 275 pc, added a dark halo component and calculated rotation curves. In Fig. 10 I show first a maximum disk model in which the scale radii and the bulge-to-disk ratio as found in the photometric model are adopted, but the mass-to-light ratio is chosen as high as allowed by the kinematical data. As can be seen in Fig. 10 hardly any dark matter is required to fit the observed rotation curve. In the lower panel I show the predicted number of spiral arms and the Q parameter. Both diagnostics are consistent with the fact that the dynamical state of the disk of NGC 2985 allows the galaxy to develop a two-armed spiral. The implied mass-to-light ratio is M/L_B = 2.0 $M_\odot/L_\odot$. This is in good agreement with the prediction of population synthesis models. NGC 2985 has a $B-R$ colour of $B-R$ = 1.1 mag. For such a colour the population synthesis models compiled by Bell & de Jong (2001) predict a mass-to-light ratio of about M/L_B = 2.8 $M_\odot/L_\odot$.

In Fig. 11 I show a submaximal disk model for the rotation curve of NGC 2985. The fit to the rotation curve, which includes now a dark matter halo contributing as much as the

© 2006 WILEY-VCH Verlag GmbH & Co. KGaA, Weinheim

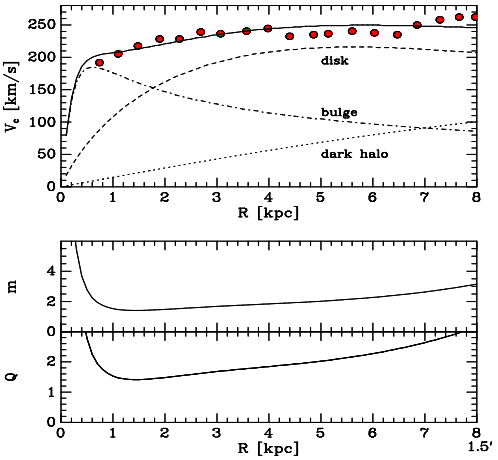

Fig. 10 Upper panel: Maximum disk model of the rotation curve of NGC 2985. The contributions by the various components are indicated as dashed lines. Lower panel: Predicted number of spiral arms m and the Toomre Q parameter. On the abscissa the scale is also indicated in arcminutes; 1.5 arcmin corresponds to the optical radius of the disk.

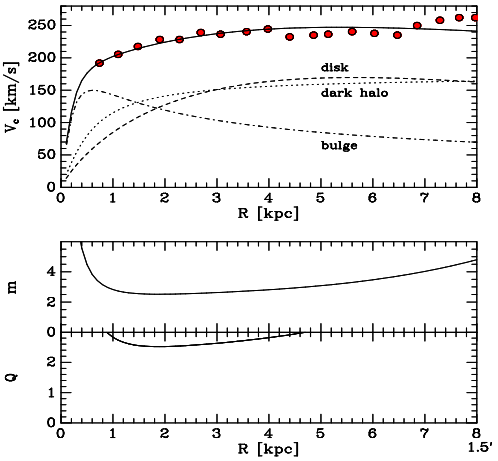

Fig. 11 Same as Fig. 10, but for a submaximal disk component.

disk, is of the same quality as in the case of a maximum disk, but both the predicted number of spiral arms and the Q parameters as well as the implied mass-to-light ratio indicate that this not viable model for the disk of NGC 2985.

6 Example: Diagnostics of the LSB galaxy F568-1

In Fuchs (2002, 2003) I have applied similar diagnostics as in the previous section to a number of low surface brightness galaxies and describe here a typical result for the example of F568-1. The image of the galaxy, reproduced from de Blok et al. (1995) in Fig. 12, shows a regular two-armed spiral pattern. The rotation curve of F568-1 has been observed by de Blok et al. (2001). Unfortunately the velocity dispersions

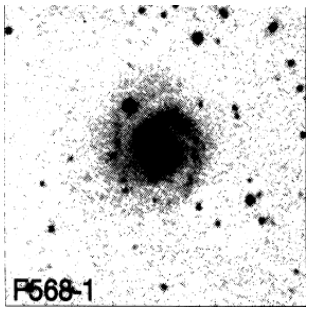

Fig. 12 Image of F568-1.

of stars in LSB disks have not been measured up to now. De Blok et al. (2001) have provided – as for each galaxy in their sample – four types of models for the rotation curve of F568-1. The first model considers only a dark halo, the next includes the contribution by the interstellar gas, and the third model adds the contribution by a stellar disk with a, according to population synthesis, 'reasonable' mass-to-light ratio of M/L_R = 1.4 $M_\odot/L_\odot$, which turns out to be a submaximal disk model. The fourth model is a maximum disk model. This suite of models is presented for the two cases that the dark halo is either a quasi-isothermal sphere or has a NFW density profile. Within each suite the reduced χ^2s are practically indistinguishable from each other. The surprising result is, when I constrain the decomposition of the rotation curve dynamically using the density wave argument discussed in section (4), I find a mass-to-light ratio of M/L_R = 14!

Lee et al.(2004) have attempted to modify the population synthesis model for LSB galaxies toaccommodate such high mass-to-light ratios. They treated the stellar population as an aging star burst with a bottom heavy IMF $\xi \sim \mathcal{M}^{-(1+\alpha)}$ (with the notation that α = 1.8 corresponds to a Salpeter law). Moreover, they varied the metallicities of the stars in the range from [Fe/H] = -2.5 to 0.4. They find that they can indeed reproduce the mass-to-light ratios and the $(B-R)_0$ colours of about 0.8 mag, which are typical for the LSB galaxies in the sample of Fuchs (2003), by adopting ages of the disks of 3 to 5 Gyrs, metallicities of [Fe/H] = -1.5 to -1, and an index of the IMF as steep as α = 2.35 to 2.85, respectively. These parameters were chosen rather ad hoc to explain the results of Fuchs (2003). However, recently Kroupa and collaborators have developed the concept of an 'integrated galactic initial mass function' which predicts very steep IMF indices α. For instance, Weidner & Kroupa (2005) predict for galactic disks with masses of several 10^{10} $M_\odot$, which I find typically for the LSBs in my sample, in their 'maximal' model an α = 2.6 (in the notation of Lee et al. 2004). The IGMF concept has not yet been adapted in detail to LSBs, but looks very promising and we hope to address this in the near future.

© 2006 WILEY-VCH Verlag GmbH & Co. KGaA, Weinheim

7 Conclusions

Imaging and spectroscopy of galactic disks allows to infer their dynamics. However, the decomposition of the rotation curves of spiral galaxies is highly degenerate and needs further constraints. These can be found by considering the implications for the dynamics of the disks of the galaxies. A useful diagnostic of the dynamics of a galactic disk is the Toomre Q stability parameter. Another diagnostic is provided by the density wave theory of galactic spiral arms which predicts the number of spiral arms. Both diagnostics can be used to constrain the masses of galactic disks. As an example of a high surface brightness spiral I have analyzed NGC 2985 along these lines and found that it seems to be dominated in the inner part, where the optical disk resides, by baryons. The resulting mass-to-light ratio is consistent with population synthesis models for such galaxies. The dynamical analysis of the disks of low surface brightness galaxies, on the other hand, implies unexpected high mass-to-light ratios. Such mass-to-light ratios can be explained by population synthesis models with a bottom heavy IMF.

References

van Albada, T.S., Bahcall, J.N., Begeman, K., Sancisi, R.: 1985, ApJ 295, 305
Arifyanto, M.I., Fuchs, B.: 2001, AGM 18, 160
Athanassoula, E., Bosma, A., Papaioannou, S.: 1987, A&A 179, 23
Bell, E.F., de Jong, R.S.: 2001, ApJ 550, 212
de Blok, W.J.G., van der Hulst, J.M., Bothun, G.D.: 1995, MNRAS 274, 235
de Blok, W.J.G., McGaugh, S.M., Rubin, V.C.: 2001, AJ 122, 2396
Bottema, R.: 1993, A&A 275, 16
Dubinski, J., Gauthier, J.-R., Widrow, L., Nickerson, S.: 2008, in: J.G Funes, E.M Corsini (eds.) Formation and Evolution of Galaxy Disks (arXiv:0802.3997)
Freeman, K.C.: 1970, ApJ 160, 811
Fuchs, B.: 1999, ASP Conf. Ser. 182, 365
Fuchs, B.: 2001, A&A 368, 107
Fuchs, B.: 2002, in: H.V. Klapdor-Kleingrothaus, R.D. Viollier (eds.) Dark matter in astro- and particle physics, Springer, Berlin, p. 28
Fuchs, B.: 2003, Ap&SS 284, 719
Fuchs, B., von Linden, S.: 1998, MNRAS 294, 513
Gerssen, J., Kuijken, K., Merrifield, M.R.: 1997, MNRAS 288, 618
Gerssen, J., Kuijken, K., Merrifield, M.R.: 2000, MNRAS 317, 545
Hockney, R.W., Hohl, F.: 1969, AJ 74, 1102
Lee, H.-y., Gibson, B.K., Flynn, C., Kawata, D. Beasley, M.A.: 2004, MNRAS 353, 113
Lindblad, B.: 1959, *Handbuch der Physik* 53, 21
Navarro, J.F. Frenk, C.S., White, S.D.M.: 1997, ApJ 490, 493
Prugniel, Ph., Zasov, A., Busarello, G., Simien, F.: 1998, A&AS 127, 117
Rubin, V.C., Ford, W.K., Thonnard, N.: 1978, ApJ 225, L107
Toomre, A.: 1964, ApJ 139, 1217
Toomre, A.: 1981, in: S.M. Fall, D. Lynden–Bell (eds.) The Structure and Evolution of Normal Galaxies, Cambridge Univ. Pres, Cambridge, p. 111
Verheijen, M.A.W., Bershady, M.A., Andersen, D.R. et al.: 2004, AN 325, 151
Weidner, C., Kroupa, P.: 2005, ApJ 625, 754

© 2006 WILEY-VCH Verlag GmbH & Co. KGaA, Weinheim